Advanced Control of a Switching Buck Regulator

Michael Elmore
Celestica Corporation
530 Columbia Drive
Johnson City, NY 13760
(607) 763-3077
FAX (607) 763-3502

Vladimir Nikulin and
Victor Skormin, Ph.D.
Watson School
Binghamton University
Binghamton, NY 13902
(607) 777-4013

Key Words

Adaptive control, Control, Converter circuits, Converter control, DC power supplies, High frequency power converters, Modeling, Power supplies, Switched-mode power supplies

Abstract

Increasing demands of electronic loads on their power supplies can be met by advanced control schemes. Model reference control of a switching buck regulator, implemented in a simulation setup, is considered and subjected to a comprehensive simulation study. This control approach results in stable operation and desired transient response of the buck converter under varying load and input voltage, and effects of parameter uncertainty and drift. The adaptation mechanism is designed utilizing the hyperstability and positivity principles. Implementation aspects are addressed.

Introduction

Switching regulators are designed to provide a stable output voltage over a wide range of loads. Passive output and input filter components, the input voltage range and the switching regulator topology all affect the stability and performance of the regulator. A good regulator specification defines the load and input voltage range and performance criteria, such as, load transient response. However, the nature of the load is not always well known, when an electronic system is first specified. Loads are often non-linear. Output distribution, including cabling and printed circuit board traces, is both resistive and inductive. System capacitance can often be a magnitude greater than the regulator output filter capacitor. Furthermore, the passive filter components in the regulator can vary with initial tolerance, temperature and electrical loading.

These wide variations in regulator and system components, output load and input voltage, can make performance specifications difficult, if not impossible, to achieve. Performance can be compromised, just to guarantee regulator stability. Designers are often forced to request specification deviations and waivers. Extra time and money can be spent in redesign, once the real requirements are understood.

A robust regulator design that would ensure its required performance over the entire range of load and environmental conditions would significantly reduce test and redesign efforts, and the cost of the final product. Performance enhancement of a power converter can be achieved by using novel components and system hardware configurations, and advanced control schemes. This study is aimed at the second approach, which has great potential due to decreasing costs of dedicated integrated circuits capable of implementation of the most sophisticated control procedures. This paper addresses such issues as modeling of power supplies, development of model reference controllers, and simulation studies of the resultant systems.

Fig. 1 shows a simplified buck regulator. Middlebrook and Cuk [1] have developed a small-signal, low frequency model of standard switching converter power topologies. The model is an average

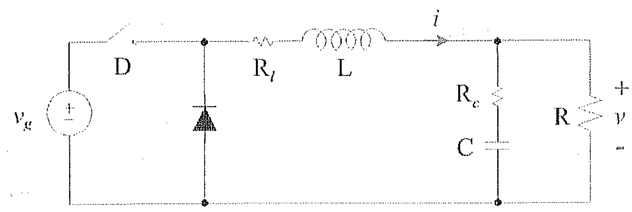

Figure 1 - Switching Buck Regulator

over one switch cycle of the two circuit states of the converter. The average model can be defined in state space form and is valid for frequencies up to 1/3 the switch frequency. Such a model can be used to investigate the effects of parameter variation, input voltage, and load variations on converter performance characteristics, such as stability, audio susceptibility and transient load response. Typical control system design approaches imply that the controlled plant is described by linear time-invariant equations. This assumption is not applicable to most power supply models. Although the models are defined by state-variable equations, parameters of these equations are dependent upon varying load and environmental conditions. This results in a high degree of uncertainty that adversely affects the ability to design efficient control systems.

The problem arising from incomplete information on the controlled plant has been addressed to some extent by adaptive control schemes [2,3,4,5]. However, more robust solutions in the form of model reference control schemes are available in modern control [6]. Such a scheme includes a reference model (RM) that represents the required performance of the buck regulator. Subjected to the same input voltage as the buck regulator, the RM generates the "model" state vector that is being compared with the "real" state vector. The discrepancy is utilized by an adaptation mechanism (AM) that defines an additional control effort, "enforcing" performance of the RM on the buck regulator regardless of the load and environmental conditions. The definition of the AM presents the central issue in the model reference control. Regardless of the actual parameter values of the buck regulator, a properly designed AM is capable of assuring that the discrepancy between its performance and the RM approaches zero with time. Mathematically, design of such an AM is consistent with the assurance that the resultant system is globally asymptotically stable. This study features the application of the hyperstability and positivity principles and the Lyapunov function technique for the definition of the AM. The results are compared and assessed from the implementation point of view.

A continuous-time, state-variable model of a buck regulator with time-dependent parameters and load is implemented in a simulation setup. Subjected to input voltage and load variations, it provides important illustrations of various problems typically observed, while working with power supplies. An analog RM and AM are also implemented in software and applied to the model of the buck regulator. Simulation experiments are conducted to select adaptation gains, investigate system robustness, stability, and sensitivity to various disturbances and initial conditions. It is shown that the application of the model reference controller can significantly improve operation of a buck regulator. The effects of output filter parameter variations on switching buck regulator performance, such as stability and load transient response, and the effects of input voltage variation on switching buck regulator audio susceptibility are eliminated. The resultant adaptive control law is suitable for implementation in a low-cost, mass-producible integrated circuit. Model reference adaptive control provides an analytical design method for switching buck regulators.

Analysis

The small signal model of the buck converter is derived from Fig. 1 with the technique of Middlebrook and Cuk. The adaptive reference model following technique is introduced and the

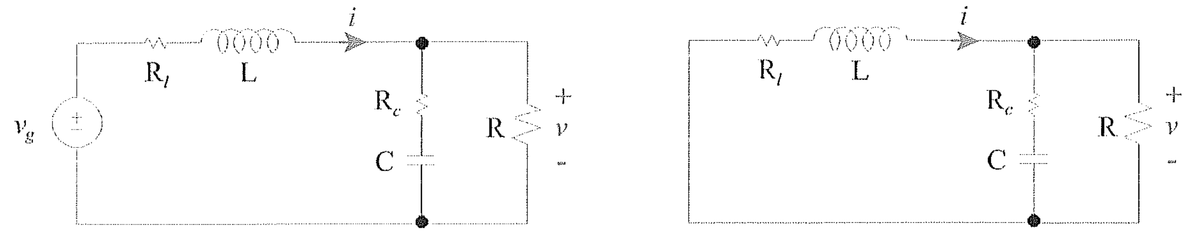

Equivalent Circuit During the On-time

Equivalent Circuit During the Off-time

Figure 2 - Equivalent Circuits for the Buck Converter

principles of hyperstability and positivity are applied to the present problem. A simulation is developed to investigate the system performance.

Averaged Small Signal State Space Model

A state space model for the buck converter shown in Fig. 1 is determined by averaging the equivalent circuits during the on-time and the off-time. The equivalent circuits are shown in Fig. 2. The state variable $\boldsymbol{x} = [i \quad v]^T$ includes the inductor current i and the voltage v across the load. It is customary to select the capacitor voltage v_c as one of the state variables. However, the capacitor voltage is not easily measured in a buck, so the load voltage is selected instead. The state space equations for the equivalent on-time circuit are given in (1) and (2). The state space equations for the equivalent off-time circuit are given in (3) and (4). Weighting each state with the duty cycle d averages the two states. (5) and (6) show the averaged states. $\mathbf{A}_1$, $\mathbf{B}_1$ and $\mathbf{C}_1$ are the state space matrices during the on-time. $\mathbf{A}_2$, $\mathbf{B}_2$ and $\mathbf{C}_2$ are the state space matrices during the off-time. Unlike the other standard switching topologies, the boost and buck-boost, $\mathbf{A}_1 = \mathbf{A}_2$ and $\mathbf{C}_1 = \mathbf{C}_2$ in the buck.

$$\frac{d}{dt}\boldsymbol{x} = \begin{bmatrix} -\frac{R_l}{L} & -\frac{1}{L} \\ \frac{L\,R - C\,R\,R_c R_l}{(R+R_c)\,L\,C} & -\frac{C\,R\,R_c + L}{(R+R_c)\,L\,C} \end{bmatrix}\boldsymbol{x} + \begin{bmatrix} \frac{1}{L} \\ \frac{R\,R_c}{(R+R_c)\,L} \end{bmatrix} v_g \tag{1}$$

$$y = [0 \quad 1]\boldsymbol{x} \tag{2}$$

$$\frac{d}{dt}\boldsymbol{x} = \begin{bmatrix} -\frac{R_l}{L} & -\frac{1}{L} \\ \frac{L\,R - C\,R\,R_c R_l}{(R+R_c)\,L\,C} & -\frac{C\,R\,R_c + L}{(R+R_c)\,L\,C} \end{bmatrix}\boldsymbol{x} + \begin{bmatrix} 0 \\ 0 \end{bmatrix} v_g \tag{3}$$

$$y = [0 \quad 1]\boldsymbol{x} \tag{4}$$

$$\frac{d}{dt}\boldsymbol{x} = \left(d\mathbf{A}_1 + (1-d)\mathbf{A}_2\right)\boldsymbol{x} + \left(d\mathbf{B}_1 + (1-d)\mathbf{B}_2\right)v_g \tag{5}$$

$$y = \left(d\mathbf{C}_1 + (1-d)\mathbf{C}_2\right)\boldsymbol{x} \tag{6}$$

Substituting (1) - (4) into (5) and (6) gives (7) and (8).

$$\frac{d}{dt}x = \begin{bmatrix} -\frac{R_l}{L} & -\frac{1}{L} \\ \frac{L\,R - C\,R\,R_c R_l}{(R+R_c)\,L\,C} & -\frac{C\,R\,R_c + L}{(R+R_c)\,L\,C} \end{bmatrix} x + \begin{bmatrix} \frac{1}{L} \\ \frac{R\,R_c}{(R+R_c)\,L} \end{bmatrix} v_g\, d \tag{7}$$

$$y = \begin{bmatrix} 0 & 1 \end{bmatrix} x \tag{8}$$

The dynamics of the buck converter are of special interest. Source voltage v_g and duty cycle d variations are introduced as $v_g = \mathbf{V}_g + \bar{v}_g$ and $d = \mathbf{D} + \bar{d}$, where $\mathbf{V}_g$ and $\mathbf{D}$ are the large signal terms and $\bar{v}_g$ and $\bar{d}$ are the time varying small signal terms. If these expressions are substituted into (7) and (8), the result is a perturbation of the state vector $x = \mathbf{X} + \bar{x}$. If the product of the $\bar{d}$ and $\bar{v}_g$ terms is ignored, the small signal terms can be separated from the large signal terms. The results are (9) and (10). The small signal model is shown in block diagram form in Fig. 3.

$$\frac{d}{dt}\bar{x} = \begin{bmatrix} -\frac{R_l}{L} & -\frac{1}{L} \\ \frac{L\,R - C\,R\,R_c R_l}{(R+R_c)\,L\,C} & -\frac{C\,R\,R_c + L}{(R+R_c)\,L\,C} \end{bmatrix} \bar{x} + \begin{bmatrix} \frac{D}{L} \\ \frac{D\,R\,R_c}{(R+R_c)\,L} \end{bmatrix} \bar{v}_g + \begin{bmatrix} \frac{V_g}{L} \\ \frac{V_g R\,R_c}{(R+R_c)\,L} \end{bmatrix} \bar{d} \tag{9}$$

$$\bar{y} = \begin{bmatrix} 0 & 1 \end{bmatrix} \bar{x} \tag{10}$$

Adaptive Model-Following Control

Adaptive model-following control (AMFC) was first applied by Landau and Courtiol [7] to force the dynamics of a subsonic aircraft, the Convair C-131 B, to take on those of a supersonic aircraft. AMFC has subsequently been implemented in a large number of advanced control systems. For example, see [6].

AMFC has its roots in earlier efforts to force a system to take on the dynamics of an ideal system using linear model-following (LMF) techniques. However, an LMF design assumes exact knowledge of system parameters. This may not always be possible or practical, since parameters can change with time or with different applications. There are also theoretical problems with LMF. Erzberger [8] showed that the structure of a system and the reference model determines whether or not it is possible to perfectly match the dynamics of a plant with the reference model. This perfect matching is called perfect model following. Chan [9] was able to show that when perfect model following conditions are not met, it is still possible to reduce steady-state errors to small values. However, exact knowledge of system parameters is still required.

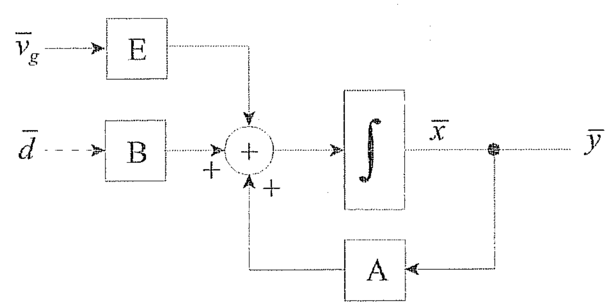

Figure 3 – Block Diagram of the Averaged Small Signal State Space Buck Model

The Erzberger conditions are not met for the buck and its reference model for perfect model following for all values of buck parameters. Nevertheless, AMFC can still be used to force the buck to follow the reference model closely. The system in Fig. 4 is described by (11) – (15).

The reference model: $$\frac{d}{dt}\bar{z} = \mathbf{A_m}\bar{z} + \mathbf{B_m}\bar{r} \qquad (11)$$

The buck: $$\frac{d}{dt}\bar{x} = \mathbf{A}\bar{x} + \mathbf{B}\,\bar{d}_1 + \mathbf{B}\,\bar{d}_2 \qquad (12)$$

The state error: $$\bar{e} = \bar{z} - \bar{x} \qquad (13)$$

The linear control signal: $$\bar{d}_1 = -\mathbf{K}\bar{x} + \mathbf{K_m}\bar{z} + \mathbf{K_u}\bar{r} \qquad (14)$$

The adaptation signal: $$\bar{d}_2 = \Delta\mathbf{K}(\bar{e},t)\,\bar{x} + \Delta\mathbf{K_u}(\bar{e},t)\,\bar{r} \qquad (15)$$

Combining (11) – (15) and grouping terms gives

$$\frac{d}{dt}\bar{e} = \left(\mathbf{A_m} - \mathbf{B}\,\mathbf{K_m}\right)\bar{e} + \left[\mathbf{Am} - \mathbf{A} + \mathbf{B}\left(\mathbf{K} - \mathbf{K_m}\right) - \mathbf{B}\,\Delta\mathbf{K}\left(\bar{v},t\right)\right]\bar{x} + \left[\mathbf{B_m} - \mathbf{B}\,\mathbf{K_u} - \mathbf{B}\,\Delta\mathbf{K_u}\left(\bar{v},t\right)\right]\bar{r}. \qquad (16)$$

If one assumes that the conditions for perfect model following exist, then one can write

$$\mathbf{A_m} - \mathbf{A} = \mathbf{B}\left(\mathbf{K_m}^0 - \mathbf{K}^0\right) \qquad (17)$$

and

$$\mathbf{B_m} = \mathbf{B}\,\mathbf{K_u}^0, \qquad (18)$$

where $\mathbf{K_u}^0$, $\mathbf{K}^0$ and $\mathbf{K_m}^0$ are the unknown values of $\mathbf{K_u}$, $\mathbf{K}$ and $\mathbf{K_m}$ that guarantee perfect model following. Substituting (17) and (18) into (16) yields

$$\frac{d}{dt}\bar{e} = \left(\mathbf{A_m} - \mathbf{B}\,\mathbf{K_m}\right)\bar{e} + \mathbf{B}\left[\mathbf{K_m}^0 - \mathbf{K_m} - \Delta\mathbf{K}\left(\bar{v},t\right)\right]\bar{x} + \mathbf{B}\left[\mathbf{K_u}^0 - \mathbf{K_u} - \Delta\mathbf{K_u}\left(\bar{v},t\right)\right]\bar{r}, \qquad (19)$$

where $\mathbf{K}^0$ and $\mathbf{K}$ have been set to 0. $\mathbf{A_m} - \mathbf{B}\,\mathbf{K_m}$ must be a Hurwitz matrix, so that the system is asymptotically stable. The feedback matrix $\mathbf{K}$ is only included in the analysis to derive the time-varying component $\Delta\mathbf{K}$. A real buck would not have the roots of its characteristic equation adjusted in this

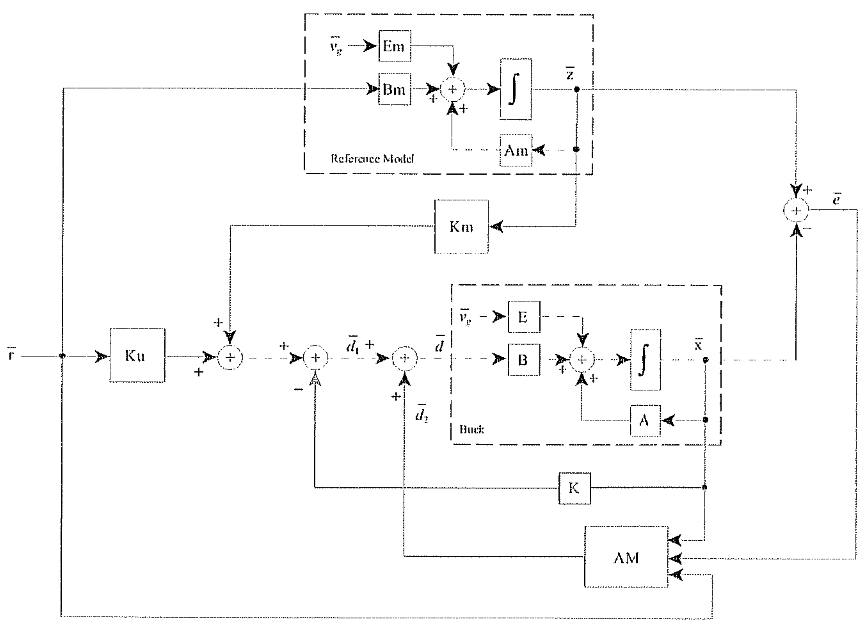

Figure 4 – Block Diagram of the Adaptive Model-Following Control for the Buck

fashion. The intent is to perform an analysis that more naturally leads to a circuit implementation.

Matrices $\mathbf{K}_m$ and $\mathbf{K}_u$ are constructed using the "best guess " values of **A** and **B**. This is necessarily the case, since the "real" buck parameters are assumed to be poorly known and changing. In a purely LMF control the accuracy of the "best guess" value is important, because it determines how well the "real" buck follows the reference model.

Hyperstability and Positivity

If a model reference adjustable system (MRAS) can be split into two blocks as shown in Fig. 5, then stability of the system can be assured. The feedback path includes a time-varying block satisfying the Popov integral inequality [6]:

$$\int_0^{t_1} \bar{v}^T \bar{w}\, dt \geq -\gamma_0^2, \tag{20}$$

for all $t_1 \geq 0$, where γ_0^2 is an arbitrary positive finite constant. If the feedforward block is constructed so that the feedback system is globally (asymptotically) stable for all feedback blocks satisfying the Popov inequality, then the feedback system is *hyperstable* and the feedforward block is a hyperstable block [6].

The conditions for the existence of a hyperstable system reside in the *positivity* properties of the feedforward block. The feedforward block must be strictly positive real. This condition can be satisfied by solving the Lyapunov equation for a filter **D** that guarantees that the feedforward block is strictly positive real [6]. From (19) comes

$$\left(\mathbf{A}_m - \mathbf{B}\mathbf{K}_m\right)^T \mathbf{P} + \mathbf{P}\left(\mathbf{A}_m - \mathbf{B}\mathbf{K}_m\right) = -\mathbf{Q}. \tag{21}$$

$$\mathbf{D} = \mathbf{B}^T\mathbf{P} \tag{22}$$

$$\bar{v} = \mathbf{D}\,\bar{e} \tag{23}$$

The equation describing the system in Fig. 5 is

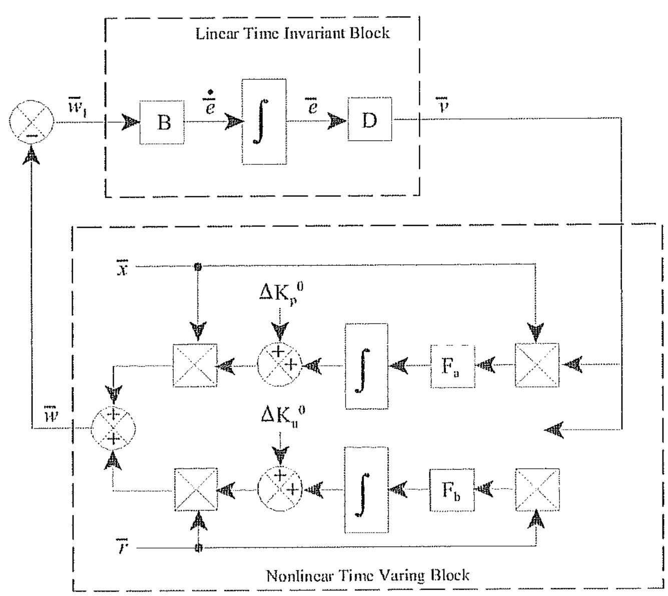

Figure 5 – Equivalent Feedback System for the MRAS

$$\frac{d}{dt}\bar{e} = \left(\mathbf{A}_m - \mathbf{B}\,\mathbf{K}_m\right)\bar{e} + \mathbf{B}\,\bar{w}_I \tag{24}$$

The adaptation law requires that $\lim_{t\to 0}\bar{e} = 0$. This implies that the adaptation mechanism has memory represented by the fundamental matrix $\mathbf{A}_m - \mathbf{B}\mathbf{K}_m$ of (24). Vector $\bar{w}_I$ in (24) is defined as:

$$\begin{aligned}\bar{w} = -\bar{w}_I &= \left[\Delta\mathbf{K}(\bar{v},t) - \mathbf{K}_m{}^0 + \mathbf{K}_m\right]\bar{x} + \left[\Delta\mathbf{K}_u(\bar{v},t) - \mathbf{K}_u{}^0 + \mathbf{K}_u\right]\bar{r} \\ &= \left[\int_0^t \Phi_I(\bar{v},t,\tau)\,d\tau + \Delta\mathbf{K}_m{}^0\right]\bar{x} + \left[\int_0^t \Psi_I(\bar{v},t,\tau)\,d\tau + \Delta\mathbf{K}_u{}^0\right]\bar{r},\end{aligned} \tag{25}$$

where

$$\Delta\mathbf{K}_m{}^0 = \mathbf{K}_m - \mathbf{K}_m{}^0 \tag{26}$$

and

$$\Delta\mathbf{K}_u{}^0 = \Delta\mathbf{K}_u(0) + \mathbf{K}_u - \mathbf{K}_u{}^0. \tag{27}$$

Proportional terms are sometimes added to (25) to increase the speed of adaptation. They are not shown here, since they are not used in the simulation.

Note that Popov integral inequality is assured by the appropriate selection of matrix-functions $\Phi_I(\bar{v},t,\tau)$ and $\Psi_I(\bar{v},t,\tau)$:

$$\Phi_I(\bar{v},t,\tau) = \mathrm{f}\,\bar{v}(\tau)\left[\mathrm{G}\,\bar{x}\right]^{\mathrm{T}}, \tag{28}$$

where f is a scalar and

$$\mathrm{G} = \begin{bmatrix} \mathrm{g}_{11} & 0 \\ 0 & \mathrm{g}_{22} \end{bmatrix} \tag{29}$$

and

$$\Psi_I(\bar{v},t,\tau) = \mathrm{h}\,\bar{v}(\tau)\,\bar{r}, \tag{30}$$

where h is a scalar.

Simulation

Mathematica 3.0 [10] and its *Control System Professional* [11] application is used to find the $\mathbf{K}_u$, $\mathbf{K}_m$ and **D** matrices in terms of the matrix elements of the system matrices of the reference model, the "best guess" and the "real" buck. Solving explicitly for the matrix elements enables numerical values to be adjusted later in the simulation without recalculation of $\mathbf{K}_u$, $\mathbf{K}_m$ and **D** in *Mathematica.* Matrix **Q** is chosen to be the identity matrix in the Lyapunov equation. The relative performance of the two components of the state variable is modified by the choice of the **Q** matrix [7]. Since the filtered steady state error $\bar{v}$ is a linear combination of $\bar{i}$ and $\bar{v}$, it is necessary to weight one of the diagonal elements of **Q** to favor $\bar{v}$. However, this results in a complicated solution of the Lyapunov equation for **P**, if the weighting term is to remain explicit. Alternatively, **D** can be multiplied by a weighting matrix to favor $\bar{v}$. This is an ad hoc approach that is justified here only by the positive results. A weighting of 10,000 is chosen. The filtered error is

$$\bar{v} = d_{11}\,\bar{i} + 10000\,d_{21}\,\bar{v}, \tag{31}$$

where d_{11} and d_{21} are the two elements of **D**.

VisSim32 [12] is used to simulate the system. The simulation construction closely follows the block diagram in Fig. 4. The $\mathbf{K}_u$, $\mathbf{K}_m$ and **D** matrices are programmed from the results of the *Mathematica* calculation. The adaptation mechanism (AM) is implemented with (25) and (28) – (30). Adaptation gains are found through trial and error. They are f = 200, g_{11} = 200, g_{22} = 2500 and h = 1250000.

Results

The simulation was run for many combinations of parameters for the reference model, "best guess" and "real" buck. Five of the more illustrative trials are shown in Table I. The trials fall into three categories: 1) disturbance to the duty cycle $\bar{d}$, 2) disturbance to the input voltage $\bar{v}_g$ and 3) disturbance to a parameter. $\bar{d}$ and $\bar{v}_g$ disturbances were in the form of a 0.1 step. Only the output load R was disturbed, since this is the parameter that is most likely to change frequently in a real power converter.

The simulation results are given in Figs. 6 – 15. The reference model output $\bar{y}_m$ is the upper waveform in each picture, also shown in red. The output $\bar{y}$ of the "real" buck is the lower waveform, shown in blue. The "real" buck waveforms have been lowered by 1.0, so that the two waveforms can be clearly distinguished. All the simulations on the left side were done without adaptation. This was accomplished by disconnecting the adaptation signal d_2 in Fig. 4. The waveforms on the right side were made with adaptation. Only the parameters shown in Table I and initial conditions on the reference model and "real" buck were changed between trials. Initial conditions on the voltage integrator needed to change, when the output load R was changed to avoid oscillations at the beginning of the simulation.

The voltage portion of the steady state error goes to zero in each simulation with adaptation, except in trial 3. Fig. 11 shows that the output of the "real" buck is slightly greater than 4.0. This is a consequence of the magnitude of the weighting factor given in (31). The voltage error could be reduced (or made larger) with an increase (or decrease) to the weighting factor. It has been determined that the voltage error can be made acceptably small. It should be pointed out that if a controlled current output were required, then one could weight **D** to favor current.

The simulation results show a remarkable robustness. Disturbances to signals and parameters do not produce any significant error and the response is rapid. The "real" buck parameters can be significantly different from the "best guess". An important point is that the duty cycle $\bar{d}$ remains bounded between 0 and 1 in all five trials.

Conclusions

It has been demonstrated through simulation that the small signal dynamics of a buck regulator

		Parameters						
		$\bar{v}_g$	$\bar{d}$	L (μH)	C (μF)	R (Ω)	R_l (Ω)	R_c (Ω)
Trial 1	Reference Model	10	0.4	10	20	1	0.004	0.1
	Best Guess Buck	10	0.4	10	30	1	0.004	0.1
	Real Buck	10	0.4	20	20	1	0.004	0.1
Trial 2	Reference Model	10	0.4	20	30	1	0.004	0.1
	Best Guess Buck	10	0.4	10	30	1	0.004	0.1
	Real Buck	10	0.4	10	30	10	0.004	0.1
Trial 3	Reference Model	10	0.4	20	30	2	0.004	0.1
	Best Guess Buck	10	0.4	10	30	1	0.004	0.1
	Real Buck	10	0.4	20	20	2□10	0.004	0.1
Trial 4	Reference Model	10	0.4	20	30	1	0.004	0.1
	Best Guess Buck	10	0.4	50	20	1	0.004	0.1
	Real Buck	10	0.4	10	10	1	0.004	0.1
Trial 5	Reference Model	10	0.4	3	200	10	0.004	0.1
	Best Guess Buck	10	0.4	10	20	10	0.004	0.1
	Real Buck	10	0.4	15	25	10□5	0.004	0.1

Table I - Parameters for Simulation Trials

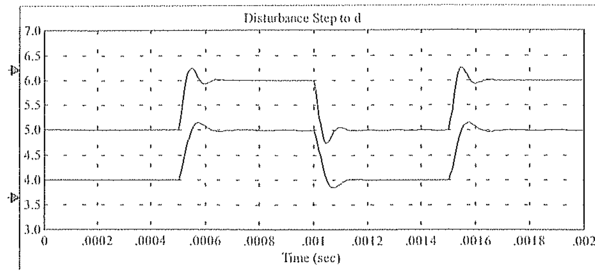

Fig. 6 - Trial 1 Without Adaptation

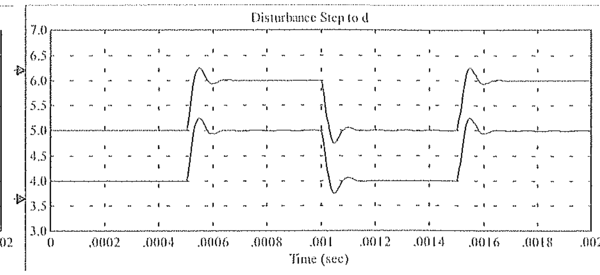

Fig. 7 - Trial 1 With Adaptation

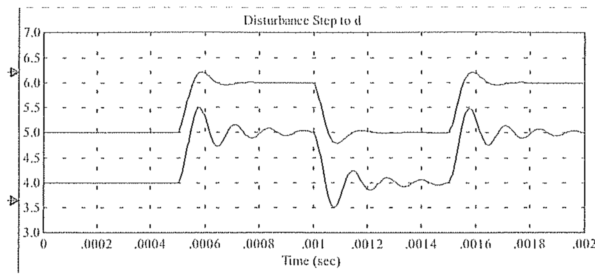

Fig. 8 - Trial 2 Without Adaptation

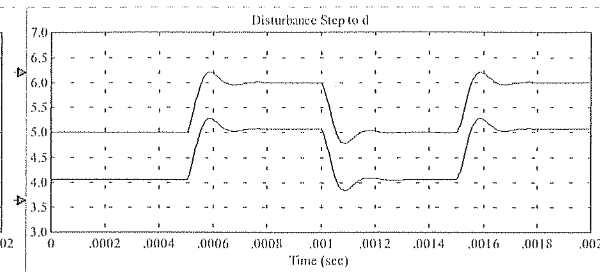

Fig. 9 - Trial 2 With Adaptation

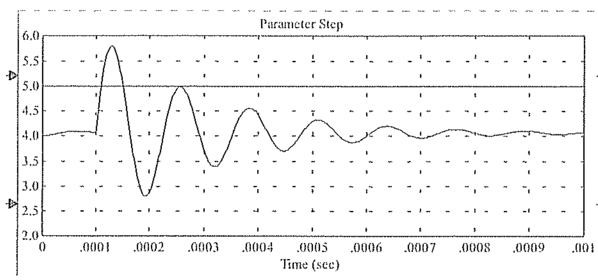

Fig. 10 - Trial 3 Without Adaptation

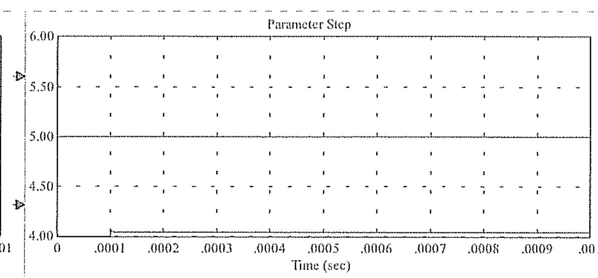

Fig. 11 - Trial 3 With Adaptation

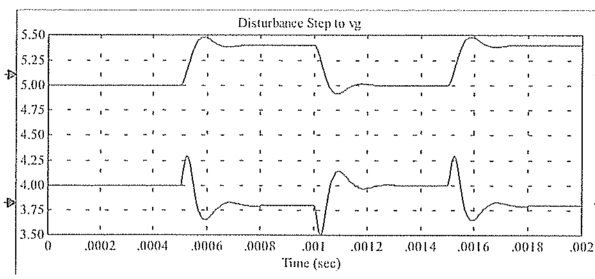

Fig. 12 - Trial 4 Without Adaptation

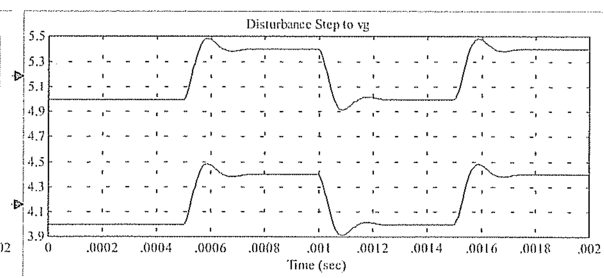

Fig. 13 - Trial 4 With Adaptation

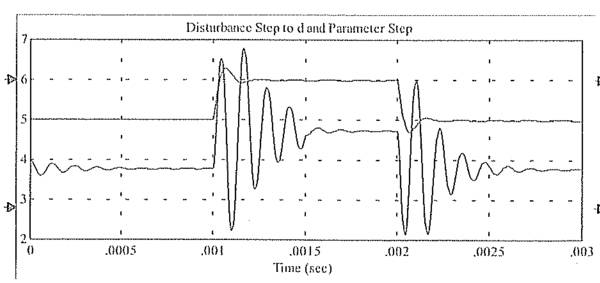

Fig. 14 Trail 5 - Without Adaptation

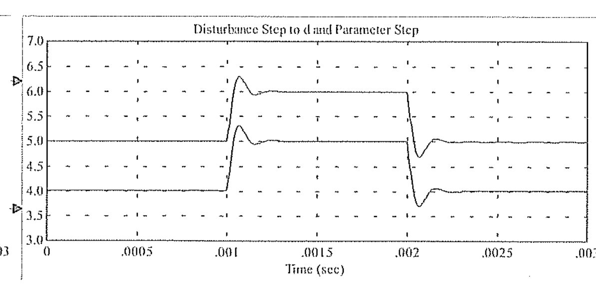

Fig. 15 - Trial 5 With Adaptation

can be made to closely follow a reference model for changes to all major parameters of the buck. These parameters include the output capacitor, the inductor and load. Parasitic parameters of the output capacitor and inductor and the input voltage and duty cycle can also be adapted. The state generalized error is a linear combination of the inductor current and output voltage errors. By weighting the error in favor of the voltage the voltage error can be made acceptably small. The buck duty cycle remains bounded between zero and one for a practical range of disturbances and parameter changes.

More work needs to be done. A circuit implementation needs to be developed. An analog approach is probably required to achieve the fast time constants investigated here. An inexpensive, "universal", integrated circuit might be developed. The reference model and gains could be programmed with a few passive, external components. This controller could be integrated with a pulse width modulator to drive the power FET. A digital realization may be possible for buck converters with longer time constants. This would provide more flexibility, but would be a more expensive approach.

AMFC offers a solution to variations in buck converter dynamics, due to parameter uncertainties and changes. However, there must be limits within which the parameters can change before undesirable effects occur. Non-linear effects, due to saturating circuit elements need to be investigated.

Work has begun on an AMFC control for a boost converter. This will be reported on at a later time.

References

1. R. D. Middlebrook and S. Cuk, "A General Unified Approach to Modelling Switching-Converter Power Stages," *IEEE Power Electronics Specialists Conference Record*, pp. 18 – 34, June 1976.
2. S. S. Kelkar and F. C. Lee, "A Novel Input filter Compensation Scheme for Switching Regulators," *Proceedings of the IEEE Power Electronics Specialists Conference and Expositions*, Cambridge, MA, pp. 260 – 271, June 14 – 17, 1982.
3. S. S. Kelkar and F. C. Lee, "Adaptive Input Filter Compensation for Switching Regulators," *IEEE Transactions on Aerospace and Electronic Systems*, vol. AES-20, no. 1, pp. 57 - 66, January 1984.
4. F. C. Lee and Y. Yu, "An Adaptive-Control Switching Buck Regulator - Implementation, Analysis and Design," *IEEE Transactions on Aerospace and Electronic Systems*, vol. AES-16, no. 1, pp. 84 - 99, January 1980.
5. Tomonobu Senjyu, Hajime Kinjo and Katsumi Uezato, "Unity Power Factor AC/DC Converter Using Full-Order State Observer, *Proceedings of the IEEE International Symposium on Industrial Electronics*, Warsaw, Poland, pp. 761 – 766, June 17 – 20, 1996.
6. Yoan D. Landau, *Adaptive Control. The Model Reference Approach*, Marcel Dekker, Inc., New York, NY, 1979.
7. Yoan D. Landau and B. Courtiol, "Design of Multivariable Adaptive Model Following Control Systems," Automatica, vol. 10, pp. 483 – 494, 1974.
8. Heinz Erzberger, "Analysis and Design of Model following Control Systems by State Space Techniques," *Proceedings of the Joint Automatic Control Conference*, pp. 572 – 581, 1968.
9. Chan, Y. T., "Perfect Model Following With a Real Model", *Proceedings of the Joint Automatic Control Conference*, pp. 287 – 293, 1973.
10. Mathematica for Students 3.0, Wolfram Research, Inc., Champaign, IL.
11. Control System Professional Ver. 1.0.0, Wolfram Research, Inc., Champaign, IL.
12. VisSim32 Ver. 2.0k, Visual Solutions, Inc., Westford, MA.